Applied Catalysis A: General 487 (2014) 165–171

Contents lists available at ScienceDirect

Applied Catalysis A: General

journal homepage: www.elsevier.com/locate/apcata

Gallium exchanged phosphotungstic acid supported on zirconia: Efficient catalyst for Friedel–Crafts benzylation

Ch. Ramesh Kumar, Srinivas M., N. Lingaiah*

Catalysis Laboratory, Inorganic & Physical Chemistry Division, CSIR-Indian Institute of Chemical Technology, Hyderabad 500 007, Telangana, India

ARTICLE INFO

Article history:
Received 14 May 2014
Received in revised form 9 September 2014
Accepted 11 September 2014
Available online 19 September 2014

Keywords:
Anisole
Benzyl alcohol
Benzylation
Gallium
Heteropoly tungstate

ABSTRACT

Gallium exchanged phosphotungstic acid (GaTPA) supported on zirconia catalysts were prepared and their physico-chemical properties were derived from FT-infrared spectra, X-ray diffraction, X-ray photoelectron spectroscopy, temperature programmed desorption of ammonia, pyridine adsorbed FT-IR spectra and solid state ^{31}P NMR spectroscopy. The catalysts activity was studied for Friedel–Crafts benzylation of anisole with benzyl alcohol. The characterization of catalysts revealed that the primary Keggin structure remained intact during exchange of TPA protons with Ga^{3+}. The exchange of Ga^{3+} with the protons of TPA led to increase in Lewis acidity. Benzylation activity depended on the amount of the GaTPA and the catalyst with 20 wt% GaTPA supported on zirconia showed highest activity. The activity profiles of the catalysts were well correlated with the characteristics of the catalysts. Reaction parameters such as effect of reaction temperature, catalyst weight, anisole to benzyl alcohol molar ratio were also optimized. Under optimized conditions complete conversion of benzyl alcohol was obtained. The catalyst is reusable with consistent activity.

© 2014 Elsevier B.V. All rights reserved.

1. Introduction

Gallium containing catalysts have attracted considerable attention due to their remarkable activity as catalysts in the Friedel–Crafts type benzylation and acylation reactions [1–3]. Recently, it has been shown that Ga_2O_3 supported on MCM-41 is very active for benzylation and acylation reactions [2,3]. Choudhary et al. also reported that the activity of the ZSM-5 and Hβ can be improved by the incorporation of Ga in the framework for benzylation of benzene [4,5]. Very recently, Anand et al. [6] reported preparation, characterization of 3D mesoporous gallosilicates and catalytic activity of these materials was investigated for benzylation of aromatic compounds.

Heteropoly acids (HPAs) have attracted significant attention because of their high acidity and favourable redox properties. Among different HPAs, Keggin type are well known and widely studied compounds for various catalytic applications due to their relatively high thermal stability, redox and acidic properties. Keggin type heteropoly anion can be represented as, $X_nM_{12}O_{40}^{(8-n)-}$, where X = heteroatom. The ratio between addenda atom and heteroatom for these compounds is 12 (M/X = 12). The heteroatom X is usually either P^{5+} or Si^{4+} and hardly ever Co^{3+}, Ge^{4+} and M is usually W^{6+} or Mo^{6+} [7,8]. The Keggin unit consists of a central atom X in tetrahedral co-ordination (XO_4) which is surrounded by 12 metal–oxygen octahedral (MO_6) units. There are four types of oxygen atoms in a Keggin unit. There are 4 central oxygen atoms (O_a), 12 oxygen atoms that bridge two metal atoms sharing a central oxygen atom (edge-sharing O_e), 12 oxygen atoms that bridge metal atoms not sharing a central oxygen atom (O_c), and 12 terminal oxygen atoms (O_t) bound to a single metal atom. These Keggin type HPAs has been the focus of considerable attention because of its catalytic activity in variety of acid catalyzed organic reactions, such as Friedel–Craft's alkylation, acylation, oxidation, hydration of alkenes, esterification, transesterification and carbonylation [9–14]. The disadvantages of HPAs are low surface area (<10 m^2/g) and high solubility in polar media. These disadvantages can be overcome by dispersing them on inorganic materials [15–17], exchanging the protons of HPAs with metal cations [18–20]. It is thought that Ga^{3+} can be used to exchange the protons of TPA to induce the catalytic properties associated with Ga along with TPA. Filek et al. [21] synthesized gallium and indium salts of the tungstophosphoric acid and catalytic performance was tested for synthesis of unsymmetrical ethers. It was observed that Ga salt of TPA showed relatively high performance in synthesis of unsymmetrical ethers compared to parent TPA and

* Corresponding author. Tel.: +91 40 27191722; fax: +91 40 27160921.
E-mail addresses: nakkalingaiah@iict.res.in, lingaiah66@yahoo.co.in (N. Lingaiah).

http://dx.doi.org/10.1016/j.apcata.2014.09.018
0926-860X/© 2014 Elsevier B.V. All rights reserved.

other metal salts such as AlTPA and InTPA. The drawback of GaTPA is its solubility in polar solvents even after exchange of TPA protons with Ga^{3+} ions.

In the present work, a series of Ga exchanged TPA supported on zirconia catalysts were prepared and characterized by different spectroscopic and non spectroscopic techniques to elucidate their physico-chemical properties. The catalysts were evaluated for benzylation of anisole with benzyl alcohol. The influence of various reaction parameters was also studied to optimize the reaction conditions.

2. Experimental

2.1. Preparation of hydrous zirconia

Hydrous zirconia was prepared by hydrolyzing the aqueous solution of $ZrOCl_2{\cdot}8H_2O$ with ammonium hydroxide at pH of 10. The precipitate was filtered off and thoroughly washed with deionized water several times until the chloride content was negligible. The precipitate was dried at 120 °C for 36 h. The hydrous zirconia after thorough drying was used as support.

2.2. Preparation of zirconia supported gallium exchanged TPA catalysts

Preparation of Ga^{3+} exchanged TPA supported on ZrO_2 involves two steps. In the first step, GaTPA was prepared by exchanging the protons of TPA with Ga^{3+}. The required quantity of TPA dissolved in minimum amount of distilled water and to this the calculated amount of aqueous $Ga(NO_3)_3$ was added drop wise. The resulting mixture was aged for 1 h at 80 °C. The excess water was evaporated to dryness. The obtained catalyst mass was oven dried at 120 °C for overnight, calcined at 300 °C for 2 h.

In the second step, GaTPA supported on zirconia were prepared by impregnation method. The required amount of GaTPA dissolved in distilled water was added to zirconia with continuous stirring. The resultant mixture was allowed to stand for 3 h and the excess water was evaporated on a water bath. The dried catalyst masses were kept overnight for further drying in an air oven at 120 °C and finally calcined at 300 °C for 2 h. The catalysts were represented as *x* wt% GaTPA/ZrO_2, where *x* represents the weight percentage of GaTPA.

2.3. Characterization of catalysts

The Fourier transform infrared (FT-IR) spectra were recorded on a Bio-rad Excalibur series spectrometer using KBr disc method.

The nature of the acid sites (Bronsted and Lewis) of the catalysts was determined by FT-IR spectroscopy with chemisorbed pyridine. The pyridine adsorption studies were carried out in the diffuse reflectance infrared Fourier transform (DRIFT) mode. Prior to the pyridine adsorption catalysts were degassed under vacuum at 200 °C for 3 h followed by suspending dry pyridine. Then, the excess pyridine was removed by heating the sample at 120 °C for 1 h. After cooling the sample to room temperature, FT-IR spectra of the pyridine-adsorbed samples were recorded.

X-ray powder diffraction patterns were recorded on a Rigaku Miniflex diffractometer using Cu K_α radiation (1.5406 Å) at 40 kV and 30 mA and secondary graphite monochromatic. The measurements were obtained in steps of 0.045° with count times of 0.5 s, in the 2θ range of 10–80°.

XPS measurements were conducted on a KRATOS AXIS 165 with a DUAL anode (Mg and Al) apparatus using an MgK_α anode. The non-monochromatized AlK_α X-ray source ($h\upsilon$ = 1486.6 eV) was operated at 12.5 kV and 16 mA. Before acquisition of the data, each sample was out gassed for approximately 3 h at 100 °C under a vacuum pressure of 13.3 μPa to minimize surface contamination. The XPS instrument was calibrated using Au as the standard. For energy calibration, the C1s photoelectron line was used. The C1s binding energy was 285 eV. Charge neutralization of 2 eV was used to balance the charge-up of the sample. The spectra were deconvoluted using Sun Solaris Vision-2 curve resolver. The location and the full width at half maximum value for the species were determined using the spectrum of a pure sample. Symmetric Gaussian shapes were used in all cases. Binding energies for identical samples were, in general, reproducible within ±0.1 eV.

^{31}P nuclear magnetic resonance (NMR) spectra of solids were recorded in a 400 MHz Bruker spectrometer. A 4.5 μs pulse (90°) was used with repetition time of 5 s between pulses in order to avoid saturation effects. Spinning rate was 5 kHz. All the measurements were carried out at room temperature using 85% H_3PO_4 as standard reference.

2.4. General alkylation reaction procedure

The alkylation reaction was carried-out in a 50 ml two-necked round bottom flask provided with a reflux condenser. In a typical run, 10 g of anisole and 3.37 g of benzyl alcohol (15:5 molar ratios) along with 0.75 wt% catalyst was taken in flask. The reaction was carried out at a reaction temperature of 120 °C. The reaction mixture was withdrawn at different intervals and analyzed by a gas chromatography equipped with a SE-30 column and flame ionization detector. The identification of products was made from GC–MS analysis.

3. Results and discussion

3.1. Catalysts characterization

Fig. 1 shows the IR spectra of GaTPA/ZrO_2 catalysts. The characteristic bands of heteropoly anion were observed in the range of 700–1100 cm^{-1}. The characteristic bands of pure TPA/$PW_{12}O_{40}{}^{3-}$ (Fig. 1h) as shown in the insert of the figure appear at 1081, 962, 910, 796 which corresponds to ν_{as}(P–O), ν_{as}(W–O_t), ν_{as}(W–O_c–W) and ν_{as}(W–O_e–W) vibrations, respectively [22]. In the case of GaTPA/ZrO_2 catalysts three characteristic bands were observed at 1084, 991 and 896 cm^{-1} and other band at 796 cm^{-1} is merged with the band related to ZrO_2. The observed characteristic bands of Keggin ion for GaTPA/ZrO_2 catalysts indicate that Keggin ion structure is stable even after exchanging the protons of TPA with Ga^{3+} ions. In the case of GaTPA supported on ZrO_2 catalysts, characteristic peaks of Keggin ion were not observed below 10 wt% loading of GaTPA due to strong absorption of zirconia in the same region. With increase in GaTPA loading from 10 to 25 wt% characteristic peaks of Keggin ion were clearly seen. These results indicate the retention of Keggin ion structure of GaTPA on zirconia.

GaTPA/ZrO_2 catalysts along with zirconia were characterized by X-ray diffraction (figure not shown). Ga^{3+} exchanged TPA showed similar diffraction peaks related to that of Keggin ion of TPA. The main diffraction peaks were noticed at 7.7°, 8.8°, 10.2°, 14.5°, 17.8°, 20.5°, 23.1°, 25.3° and 37.5° correspond to monoclinic phase of GaTPA, which were coincided with those reported in the literature [21]. No diffraction peaks related to $Ga(NO_3)_3{\cdot}8H_2O$ and Ga_2O_3 were observed. This indicates that the protons of TPA were exchanged with Ga^{3+} ions. These results suggest that retention of Keggin ion structure in Ga^{3+} exchanged TPA catalyst. The support zirconia showed amorphous behaviour. No crystalline phases were observed for the GaTPA/ZrO_2 samples. XRD patterns related to Keggin ion structure of heteropoly acid and it decomposition products were absent in all the catalysts. However, peaks related to Keggin ion were clearly seen in IR spectra of GaTPA/ZrO_2 catalysts which

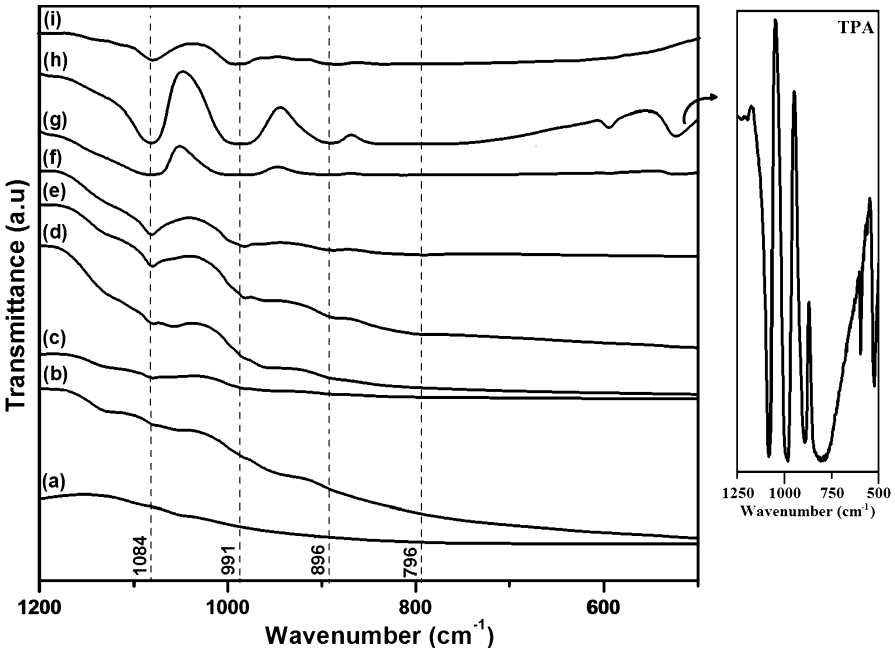

Fig. 1. FT-IR spectra of (a) ZrO_2, (b) 5 wt% GaTPA/ZrO_2, (c) 10 wt% GaTPA/ZrO_2, (d) 15 wt% GaTPA/ZrO_2, (e) 20 wt% GaTPA/ZrO_2, (f) 25 wt% GaTPA/ZrO_2, (g) GaTPA, (h) TPA and (i) 20 wt% GaTPA/ZrO_2 (used) catalysts.

confirm the retention of Keggin ion in all the catalysts. The absence of diffraction lines of Keggin ion in the XRD patterns was might be due to high dispersion of GaTPA on amorphous zirconia surface. Similar observations were made by Devassy et al. [23] for silicotungstic acid supported on zirconia. From the FT-IR and XRD patterns it can be concluded that Keggin ion of GaTPA is present on ZrO_2.

Fig. 2A shows the X-ray photoelectron spectra of Zr 3d, O 1s, W 4f, P 2p and Ga 3d of the 20 wt% GaTPA/ZrO_2 catalyst along with the binding energy values. XPS of Zr 3d deconvoluted into two peaks arising due to spin orbit splitting. The binding energies at 182.3 eV and 184.5 eV corresponds to Zr $3d_{5/2}$ and Zr $3d_{3/2}$ respectively (Fig. 2A-a). However, pure zirconia showed B.E of 181.7 and 183.3 eV corresponding to $3d_{5/2}$ and 3d3/2, respectively (Fig. 2B-b) [24]. The binding energy of Zr 3d increased accordingly compared to pure zirconia after impregnating GaTPA on ZrO_2.

The O 1s binding energies of pure ZrO_2 was observed at 531.0 and 532.8 eV (Fig. 2B-a) [24]. However, for 20 wt% GaTPA/ZrO_2 the binding energy region of O 1s observed at 530.7 and 532.1 eV. The B.E at 530.7 eV is attributed to oxygen present in W–O–W, and another peak at 532.1 eV is ascribed to the oxygen of W–O–P of the catalyst [19]. The binding energy values of W 4f are in agreement with that of pure TPA (Fig. 2C-a).

TPA showed W 4f binding energies at 35.6 eV and 37.7 eV were related to $W4f_{7/2}$ and $W4f_{5/2}$, characteristic peaks of W (VI) oxidation state (Fig. 2C-b) [25]. Impregnating GaTPA on zirconia the W 4f binding energy values of W $4f_{7/2}$ and W $4f_{5/2}$ were shifted to 36.5 eV and 38.6 eV respectively compared to TPA (Fig. 2A-c). This confirms the interaction between the Keggin unit of GaTPA and ZrO_2. The binding energy values of P 2p at 134.9 and 136.1 eV confirm the presence of P in 5+ oxidation state (Fig. 2A-d). Two binding energies were observed for Ga 3d at 22.3 and 22.6 eV related to $3d_{5/2}$ and $3d_{3/2}$ respectively (Fig. 2A-e). These B.E values of Ga suggest the presence of Ga^{3+} [26].

^{31}P solid state NMR spectroscopic studies allow in identifying the various types of species and purity of the sample. Fig. 3 shows the ^{31}P NMR spectra of 20 wt% GaTPA/ZrO_2 catalyst. From the literature it can be noticed that ^{31}P NMR signal of crystalline bulk TPA observed at −15.5 ppm corresponding to the four co-ordinated phosphorous was located in the centre of Keggin anion of heteropoly tungstate [27,28]. In the case of ^{31}P NMR of 20 wt% GaTPA/ZrO_2 catalyst characteristic signal of ^{31}P is slightly shifted to −15.69 ppm with high intensity indicates the retention of Keggin ion structure of heteropoly tungstate on zirconia. Apart from the main peak at −15.69 ppm, another minor shoulder peak was observed at −13.89 ppm, which might be due to the interaction of the Keggin units of GaTPA with zirconia support [13].

Pyridine adsorption technique is the most frequent technique from which one can detect the available Lewis and Bronsted sites on the solid acid surfaces. Fig. 4 shows the pyridine adsorbed spectra of GaTPA/ZrO_2 catalysts along with TPA, GaTPA and TPA/ZrO_2. The spectra of Ga containing catalysts showed bands at 1440 and 1537 cm^{-1} corresponding to pyridine adsorbed on Lewis and Bronsted acidic sites respectively available on the catalyst surface [19]. The band at 1486 cm^{-1} was related to pyridine adsorbed on Lewis and Bronsted acidic sites. At lower loadings of GaTPA on zirconia, the intensity of these bands was very low and an increase in these bands was observed with increase in GaTPA loading.

Similarly, pyridine adsorbed FT-IR spectrum of 20 wt% TPA/ZrO_2 catalyst also showed bands related to Bronsted and Lewis acidic sites. The Lewis acidity and Bronsted acidic sites might be originated from zirconia support and TPA respectively. However, the intensity of the combined and Lewis acidic site bands were relatively low compared to the bands of 20 wt% GaTPA on zirconia. The high intense bands of Lewis acidic sites in the case of 20 wt% GaTPA/ZrO_2 is mainly due to presence of Ga^{3+}.

3.2. Catalytic activity results

The catalysts with varying GaTPA content on ZrO_2 and 20 wt% TPA/ZrO_2 were evaluated for liquid phase benzylation of anisole with benzyl alcohol and the results are presented in Fig. 5. Catalysts with 5 wt% GaTPA exhibited only 5% conversion of benzyl alcohol with 50% selectivity towards dibenzylether. Further increase in GaTPA loading on zirconia, conversion of benzyl alcohol increased and reached about 95% for the catalyst with 20 wt% GaTPA on zirconia. Above this loading there was no appreciable variation in the conversion. The dramatic increase in activity from the 15 to 20 wt%

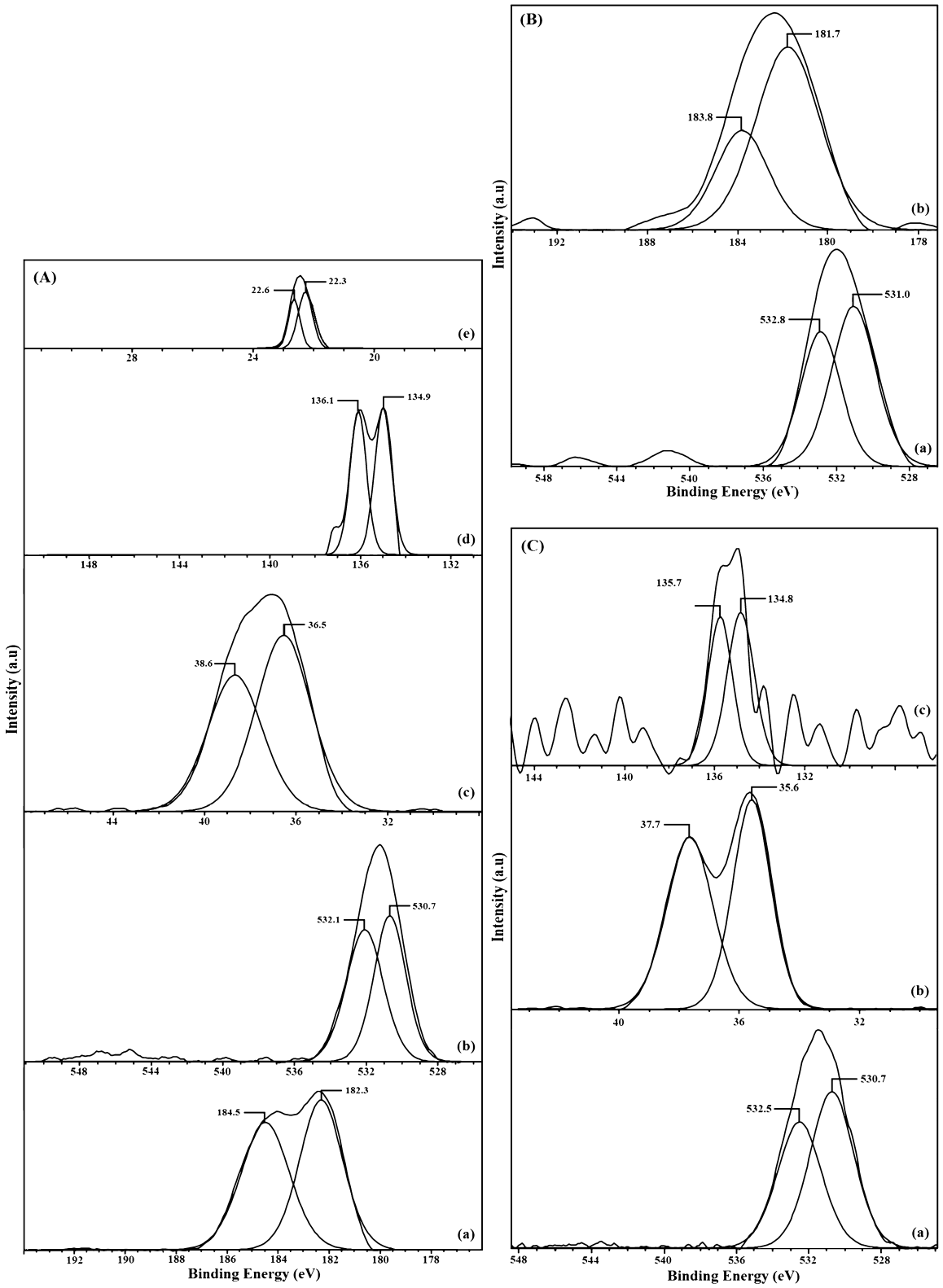

Fig. 2. X-ray photoelectron spectra of (A) 20 wt% GaTPA/ZrO_2 catalyst (a) Zr 3d, (b) O 1s, (c) W 4f, (d) P 2p, and (e) Ga 3d. (B) ZrO_2 (a) O 1s, (b) Zr 3d. (C) TPA (a) O 1s, (b) W 4f, and (c) P 2p.

of GaTPA on ZrO_2 is might be due to the well dispersed GaTPA on zirconia. XRD patterns (figure not shown) suggest the well dispersed GaTPA as XRD patterns related to GaTPA Keggin ion were absent. The observed activity can be related to the catalysts acidic functionality. The 15 and 20%GaTPA/ZrO_2 showed acidity values as 0.598 and 0.703 mmol respectively. The increase in activity for 20%GaTPA/ZrO_2 is related to its high acidity which in turn related to the content of GaTPA and its dispersion on ZrO_2.

The catalytic activity of the 20 wt% GaTPA/ZrO_2 was compared with 20 wt% TPA/ZrO_2 to know the role of Ga for this reaction.

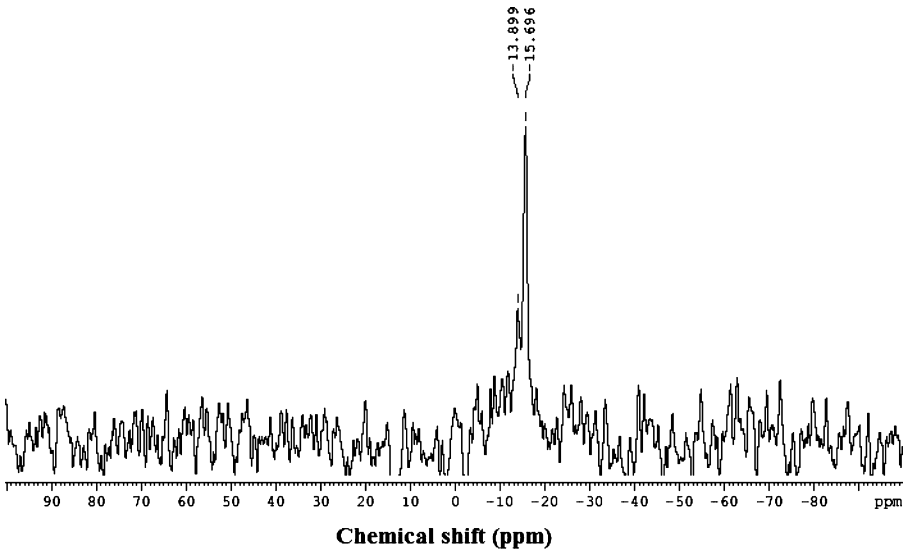

Fig. 3. Solid state ^{31}P NMR spectra of 20 wt% GaTPA/ZrO_2 catalyst.

Catalyst without Ga showed about 85% conversion of benzyl alcohol. Selectivity of the benzylated and dehydration products was found to be 76 and 24% respectively. In the case of catalyst with Ga (20 wt% GaTPA/ZrO_2), conversion of benzyl alcohol was 95% and selectivity towards benzylated product was 83%. The presence of Ga in TPA not only increased the conversion but also selectivity. Moreover, the stability of the GaTPA/ZrO_2 catalyst is high compared to TPA/ZrO_2. The high activity of the GaTPA/ZrO_2 might be due to presence of Lewis acidity associated with Ga^{3+} in the catalyst. The catalysts with Lewis acidity are known for their activity towards benzylation reaction [19,29–31].

3.3. Optimization of reaction parameters

3.3.1. Effect of catalyst weight

Catalyst concentration in the reaction mixture is an important criterion that needs to be optimized for better yield of benzylated products. The effect of catalyst amount on the conversion of benzyl alcohol was studied (figure not shown). From the results it was observed that with increase in catalyst loading from 0.37 to 1.49 wt%, conversion of benzyl alcohol increased from 8 to 95% and yield towards benzylated products also increased from 63 to 83%. This is obvious because of the proportional increase in the number of active sites. Beyond the catalyst loading of 0.75 wt%, there was no marginal change in the conversion of benzyl alcohol. However, formation of by-product was increased with increase in catalyst loading. This might be owing to rate of dehydration of benzyl alcohol is faster than the benzylation.

3.3.2. Influence of molar ratio

Molar ratio of reactants is one of the important parameters that affect the conversion of benzyl alcohol. Fig. 6 shows the influence of molar ratios on the conversion of benzyl alcohol and selectivity to benzylated product. The conversion of benzyl alcohol increased with increase in molar ratio of anisole to benzyl

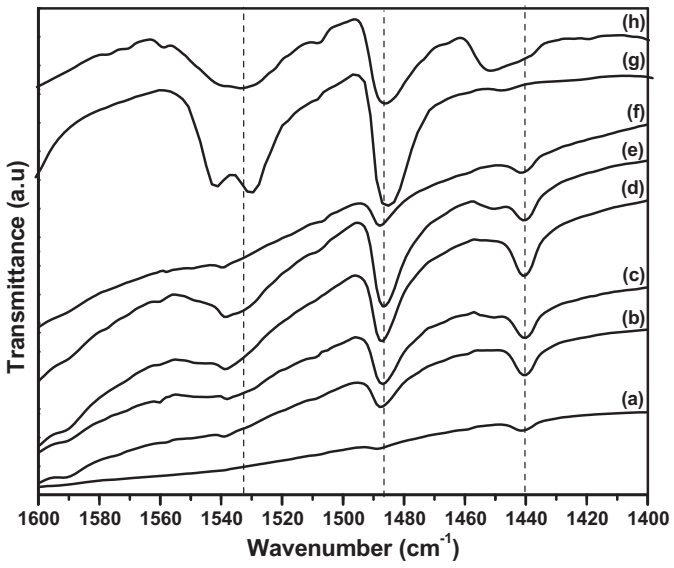

Fig. 4. Pyridine adsorbed FT-IR spectra of (a) 5 wt% GaTPA/ZrO_2, (b) 10 wt% GaTPA/ZrO_2, (c) 15 wt% GaTPA/ZrO_2, (d) 20 wt% GaTPA/ZrO_2, (e) 25 wt% GaTPA/ZrO_2, (f) 20 wt% TPA/ZrO_2, (g) TPA and (h) GaTPA catalysts.

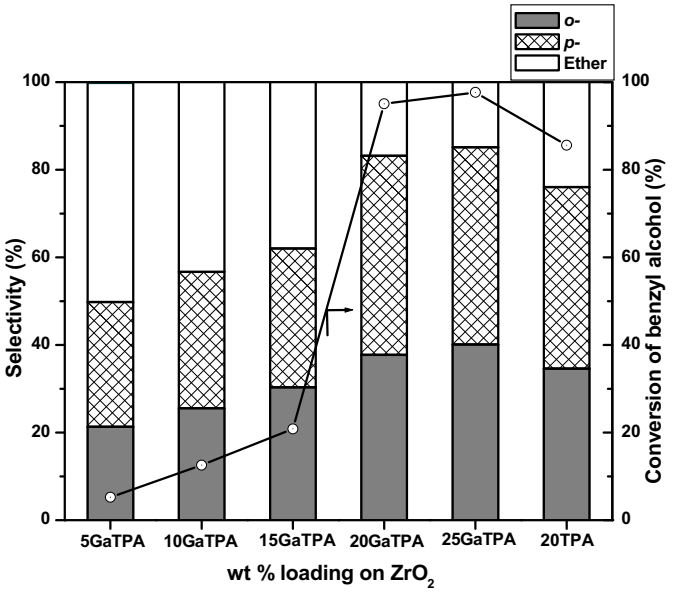

Fig. 5. Effect of GaTPA loading on zirconia on the activity of benzylation of anisole. (Reaction conditions: anisole 10 g, benzyl alcohol 3.337 g, catalyst weight 0.75 wt%, reaction temperature 120 °C, reaction time 1.5 h).

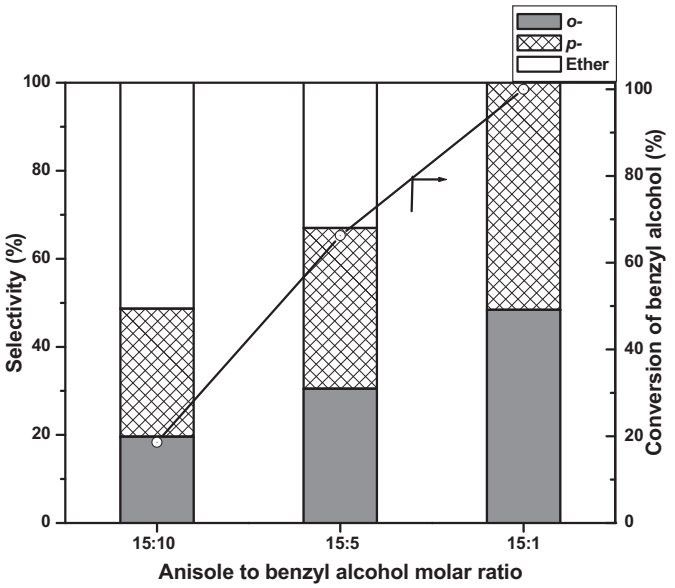

Fig. 6. The influence of anisole to benzyl alcohol molar ratio on benzylation activity over 20 wt% GaTPA/ZrO_2 catalyst. (Reaction conditions: catalyst weight 0.75 wt%, reaction temperature 120 °C, reaction time 1 h).

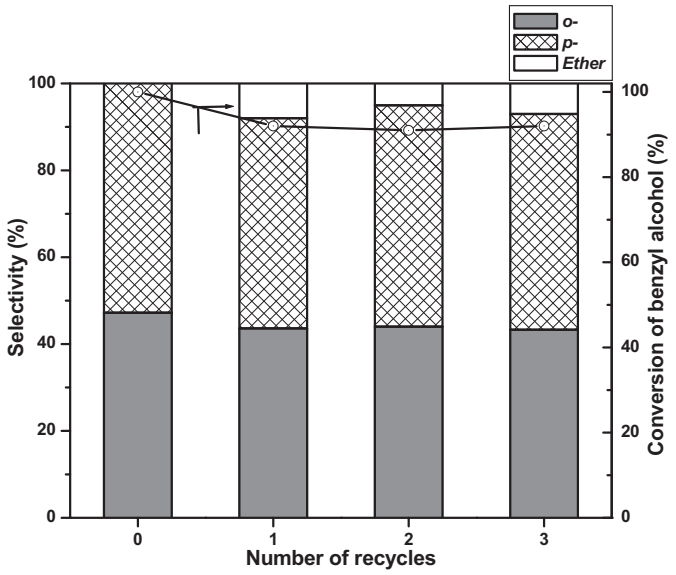

Fig. 8. Reusability of 20 wt% GaTPA/ZrO_2 catalyst during benzylation of anisole. (Reaction conditions: anisole 10 g, benzyl alcohol 3.337 g, catalyst weight 0.75 wt%, reaction temperature 120 °C, reaction time 1.5 h).

alcohol from 15:10 to 15:1. Selectivity towards benzylated product also improved from 49 to 100% with increase in anisole to benzyl alcohol molar ratio. Formation of dibenzylether (dehydration product) was expected with high benzyl alcohol concentration due to relatively low rates of benzylation compared to that of dehydration reaction [32,33].

3.3.3. Effect of reaction temperature

The effect of reaction temperature on benzylation of anisole with benzyl alcohol was studied in the range of 80–140 °C and results are presented in Fig. 7. The results suggest that the conversion of benzyl alcohol and benzylated product yield was low at a reaction temperature of 80–100 °C. The conversion increased to 95% with increase in temperature to 120 °C. Further increase in the temperature to 140 °C, complete conversion of benzyl alcohol was observed and there was no formation of any by-product. The selectivity towards benzylated product increased with increase in reaction temperature. These results suggest that a reaction temperature of 140 °C is optimum for benzylation of anisole over 20 wt% GaTPA/ZrO_2 catalyst.

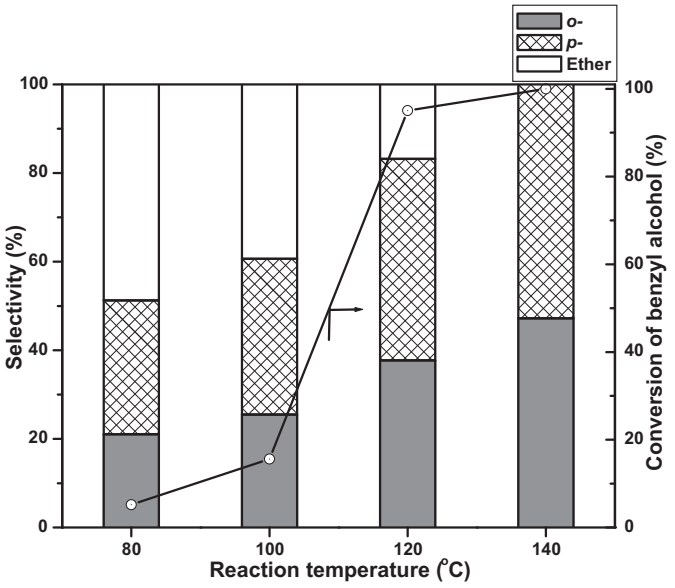

Fig. 7. Effect of reaction temperature on the benzylation of anisole over 20 wt% GaTPA/ZrO_2 catalyst. (Reaction conditions: anisole 10 g, benzyl alcohol 3.337 g, catalyst weight 0.75 wt%, reaction time 1.5 h).

3.3.4. Catalyst reusability study

In order to find the reusability of most active 20 wt% GaTPA/ZrO_2 catalyst, it was recovered by simple filtration after completion of the reaction. The recovered catalyst was washed with ethyl acetate and dried in an oven at 120 °C for 2 h. The catalyst was reused for benzylation of anisole reaction and was subjected to three cycles. The results are shown in Fig. 8. From the figure it can be observed that, in the first recycle about 8% decrease in the conversion of benzyl alcohol was observed. In the second and third recycles conversion of benzyl alcohol was almost constant. The selectivity towards benzylated products was 92% in the first recycle. However, small amount of dibenzylether (by-product) was observed in the first, second and third recycles. The selectivity towards benzylated products was consistent for every recycle of the catalyst. The used catalyst was characterized by FT-IR and the spectrum was shown in Fig. 1i. The used catalysts showed similar spectra as that of virgin catalyst and suggest that there was no change in the structure of the catalysts during reaction. These results clearly indicate the efficiency and reusability of the catalyst.

4. Conclusions

Ga exchanged TPA supported on zirconia catalysts were prepared with retention of Keggin ion structure. Generation of Lewis acid sites were possible with the exchange of protons of TPA with Ga^{3+}. Friedel–Crafts benzylation of anisole activity depends on the GaTPA loading on zirconia. Catalyst with 20 wt% of GaTPA calcined at 300 °C exhibited 100% benzyl alcohol conversion and selectivity towards benzylated products of anisole, under optimized conditions. The catalyst was reusable without any considerable loss in the activity.

Acknowledgements

The authors thank Council of Scientific & Industrial Research (CSIR) for financial support under 12th Five Year Programme project – CSC-0125. ChRK thanks CSIR, India for the award of Senior Research Fellowship.

References

[1] P. Srinivasu, A. Vinu, Chem. Eur. J. 14 (2008) 3553–3561.
[2] D. Freeman, R.P.K. Wells, G.J. Hutchings, Chem. Commun. 175 (2001) 4–1755.
[3] V.R. Choudhary, S.K. jana, B.P. Kiran, J. Catal. 192 (2000) 257–261.
[4] V.R. Choudhary, S.K. Jana, N.S. Patil, S.K. Bhargava, Micropor. Mesopor. Mater. 57 (2003) 21–35.
[5] V.R. Choudhary, S.K. Jana, A.S. Mamman, Micropor. Mesopor. Mater. 56 (2002) 65–71.
[6] C. Anand, B. Sathyaseelan, L. Samie, A. Beitollahi, R. Pradeep Kumar, M. Palanichamy, V. Murugesan, E.R. Kenawy, S.S.A. Deyab, A. Vinu, Micropor. Mesopor. Mater. 134 (2010) 87–92.
[7] J. Berzelius, Poggend. Ann. Phys. Chem. 6 (1826) 369–392.
[8] J.F. Keggin, Proc. Roy. Soc. A 144 (1934) 75–100.
[9] N. Azizi, F. Arynasab, M.R. Saidi, Org. Biomol. Chem. 4 (2006) 4275–4277.
[10] G.D. Yadav, A.R. Yadav, Ind. Eng. Chem. Res. 52 (2013) 10627–10636.
[11] P.S.N. Rao, K.T.V. Rao, P.S. Sai Prasad, N. Lingaiah, Chin. J. Catal. 32 (2011) 1719–1726.
[12] T. Okuhara, Chem. Rev. 102 (2002) 3641–3666.
[13] F. Su, L. Ma, Y. Guo, W. Li, Catal. Sci. Technol. 2 (2012) 2367–2374.
[14] K. Jagadeeswaraiah, Ch. Ramesh Kumar, P.S. Sai Prasad, N. Lingaiah, Catal. Sci. Technol. (2014), http://dx.doi.org/10.1039/C4CY00253A.
[15] N. Mizuno, M. Misono, Chem. Rev. 98 (1998) 199–217.
[16] Y. Guo, K. Li, X. Yu, J.H. Clark, Appl. Catal. B 81 (2008) 182–191.
[17] D.P. Sawant, J. Justus, V.V. Balasubramanian, K. Ariga, P. Srinivasu, S. Velmathi, S.B. Halligudi, A. Vinu, Chem. Eur. J. 14 (2008) 3200–3212.
[18] K. Shimizu, H. Furukawa, N. Kobayashi, Y. Itaya, A. Satsuma, Green Chem. 11 (2009) 1627–1632.
[19] Ch. Ramesh Kumar, K. Jagadeeswaraiah, P.S. Sai Prasad, N. Lingaiah, ChemCatChem 4 (2012) 1360–1367.
[20] K. Srilatha, S. Rekha, B.L.A. Prabhavathi Devi, P.S. Sai Prasad, R.B.N. Prasad, N. Lingaiah, Bioresour. Technol. 116 (2012) 53–57.
[21] U. Filek, D. Mucha, M. Hunger, B. Sulikowski, Catal. Commun. 30 (2013) 19–22.
[22] C.F. Oliveira, L.M. Dezaneti, F.A.C. Garcia, J.L. de Macedo, J.A. Dias, S.C.L. Dias, K.S.P. Alvim, Appl. Catal. A 372 (2010) 153–161.
[23] B.M. Devassy, S.B. Halligudi, J. Catal. 236 (2005) 313–323.
[24] M. Qing, Y. Yang, B. Wu, J. Xu, C. Zhang, P. Gao, Y. Li, J. Catal. 279 (2011) 111–122.
[25] L. Xu, W. Li, J. Hu, K. Li, X. Yang, F. Ma, Y. Guo, X. Yu, Y. Guo, J. Mater. Chem. 19 (2009) 8571–8579.
[26] B. Xu, B. Zheng, W. Hua, Y. Yue, Z. Gao, J. Catal. 239 (2006) 470–477.
[27] T. Okuhara, H. Watanabe, T. Nishimura, K. Inumaru, M. Misono, Chem. Mater. 12 (2000) 2230–2238.
[28] M. Caiado, A. Machado, R.N. Santos, I. Matos, I.M. Fonseca, A.M. Ramos, J. Vital, A.A. Valentec, J.E. Castanheiro, Appl. Catal. A 451 (2013) 36–42.
[29] K. Shimizu, K. Niimi, A. Satsuma, Appl. Catal. A 349 (2008) 1–5.
[30] P. Topka, J. Karban, K. Soukup, K. Jiratova, O. Solcova, Chem. Eng. J. 168 (2011) 433–440.
[31] Ch. Ramesh Kumar, K.T. Venkateswara Rao, P.S. Sai Prasad, N. Lingaiah, J. Mol. Catal. A 337 (2011) 17–24.
[32] Ch. Ramesh Kumar, P.S. Sai Prasad, N. Lingaiah, J. Mol. Catal. A 350 (2011) 83–90.
[33] A.B. Deshpande, A.R. Bajpai, S.D. Samant, Appl. Catal. A 209 (2001) 229–235.